# Experimental Study on Chemical Behaviors of Non-Metal Impurities in Pb, Pb-Bi and Pb-Li by Temperature Programmed Desorption Mass Spectrometer Analysis*)

Masatoshi KONDO, Yuu NAKAJIMA[1)], Teruya TANAKA[2)], Takashi NOZAWA[3)] and Takehiko YOKOMINE[4)]

*Tokyo Institute of Technology, 2-12-1 O-okayama, Meguro-ku, Tokyo 152-8550, Japan*
[1)]*Tokai University, 4-1-1 Kitakaname, Hiratsuka-shi, Kanagawa 259-1292, Japan*
[2)]*National Institute for Fusion Science, Toki, Gifu 502-5292, Japan*
[3)]*National Institute for Quantum and Radiological Science and Technology, 2-166 Omotedate, Obuchi, Rokkasho, Aomori 039-3212, Japan*
[4)]*Kyoto University, Kyotodaigaku-Katsura, Kyoto 615-8540, Japan*

(Received 22 November 2015 / Accepted 1 April 2016)

The chemical behaviors of non-metal impurities such as $O_2$, $H_2$, $N_2$, $H_2O$, $CO_2$ and CO in lead (Pb) metal, lead-bismuth (Pb-Bi) alloy and lead-lithium (Pb-Li) alloys were experimentally investigated by means of temperature programmed desorption mass spectrometer (TPD-MS) analysis. Desorption of $H_2O$ and $CO_2$ from the Pb metal and the Pb-Bi alloy was clearly detected by TPD-MS analysis. However, desorption of $H_2O$ and $CO_2$ from the Pb-Li alloys was much less than that from the Pb metal and the Pb-Bi alloy, since these molecules are chemically unstable and react with Li in the Pb-Li alloys. Then, oxygen and hydrogen must be dissolved in Pb-Li alloys as they form the chemical compounds of Li (*i.e.*, $Li_2O$, LiOH and LiH). Large desorption of hydrogen from solid Pb-Li alloys by their heating was detected. The possible mechanism for the large desorption of hydrogen from the Pb-Li alloys is based on the decomposition of LiH and Pb-Li-H at high temperature. The chemical behaviors of the non-metal impurities in the Pb-Li alloys was modeled based on the thermodynamic stability. The methodologies for the fabrication of high-purity Pb-Li alloys and the control of the impurity condition are discussed.



Keywords: liquid blanket, liquid breeder, liquid metal, non-metal impurity, temperature programmed desorption mass spectrometer

DOI: 10.1585/pfr.11.2405076

## 1. Introduction

Liquid lead-lithium (Pb-Li) alloy is one of the candidates of the tritium breeders of fusion reactors. The chemical compatibility of the Pb-Li alloy with candidate structural materials [1, 2] and the chemical behavior of tritium in the alloy [3, 4] are important issues. It is known that the chemical characteristics of liquid metals are determined by the impurities dissolved in the metals. For example, the corrosion of steels in liquid Li is influenced by oxygen [1], carbon [5] and nitrogen [6] dissolved in the melt. The corrosion mechanism of the steels in lead-bismuth (Pb-Bi) alloy [7, 8] changes by the oxygen potential in the alloy [9, 10]. The solubility data of hydrogen isotopes in the Pb-Li alloy are dispersed widely [11], and the one of the possible causes must be the difference of impurity conditions of the alloy. However, the information about the impurity control of the Pb-Li alloy is quite limited.

In the previous study, Pb-Li alloys having a various Li concentrations were fabricated by means of the mixing and the melting of small Pb and Li grains [12]. The thermal properties such as the vapor pressure [13] and the thermal conductivity at high temperature up to 873 K [14] have been investigated using the Pb-Li alloys fabricated by authors [12].

It is essential to understand the chemical behaviors of non-metal impurities such as hydrogen ($H_2$), oxygen ($O_2$), nitrogen ($N_2$), carbon dioxide ($CO_2$), carbon monoxide (CO) and moisture ($H_2O$) in Pb-Li alloy for the impurity control of the alloy. However, the methodology to evaluate the chemical behaviors of non-metal impurities dissolved in the alloy is not made clear so far. The temperature programmed desorption mass spectrometer (TPD-MS) analysis is one of the effective way to know the chemical behavior of the non-metal impurities in the alloy [15]. However, the information about the non-metal impurities dissolved in Pb-Li alloy is quite limited.

The purpose of the present study is to make clear the

*author's e-mail: kondo.masatoshi@lane.iir.titech.ac.jp*
*) This article is based on the presentation at the 25th International Toki Conference (ITC25).

Table 1 Test materials for TPD-MS analysis.

| Test material | Purity | Sample quantity [g] |
|---|---|---|
| Pb (Low purity) [12] | 99.9 % (Presence of PbO on surface of grains) | 100 |
| Pb (high purity) [12] | 99.999 % | 100 |
| LBE | 44.5Pb-55.5Bi | 100 |
| Pb-17Li (Type (A)) [12] | Li (99 %) + Pb (99.999 %) | 100 |
| Pb-17Li (Type (B)) | Li (99 %) + Pb (99.9 %)<br>(fabricated after baking procedure of Pb grains at 523 K for 90 min) | 1 |
| Pb-28Li (Type (A)) [12] | Li (99 %) + Pb (99.999 %) | 100 |

chemical behaviors of the non-metal impurities such as $H_2$, $O_2$, $N_2$, $CO_2$, CO and $H_2O$ in Pb metal and Pb alloys by means of TPD-MS analysis. The analysis was performed with Pb metal, lead-bismuth eutectic alloy (45.5Pb-55.5Bi), Pb-17Li alloy [12] and Pb-28Li alloy [12].

# 2. Experimental Conditions

## 2.1 Test materials for TPD-MS

The test materials used for the TPD-MS analysis are listed in Table 1. Two types of Pb grains with different purity grades were prepared. The diameter of these Pb grains was approximately 2.5 mm. The Pb grains having a purity of 99.999 % were supplied from Furuuchi Chemical Co. The Pb grains having a purity of 99.9 % were supplied from KOJUNDO CHEMICAL LABORATORY CO., LTD. The purity of the Li grains is 99 %. It was found in the previous study [12] that the low-purity Pb grains have the oxide layers on their surfaces, though the high-purity Pb grains do not have the oxide layer.

The Pb-17Li alloys were fabricated by the melting and the mixing of Li and Pb grains. The detail information for the fabrication procedure of the Pb-Li alloys was reported in ref. [12]. The type (A) Pb-17Li and Pb-28Li alloys were fabricated using the Pb grains, which have a purity of 99.999 %. The type (B) Pb-17Li was fabricated using the Pb grains having a purity of 99.9 %. The type (A) Pb-17Li alloy was fabricated without any pretreatments of the raw materials. The type (B) Pb-17Li alloy was fabricated after the baking procedure of the Pb grains at 523 K for 90 min to remove the surface water from the grains.

The chemical reactions between Li and Pb grains involving the non-metal impurities during the fabrication procedure were investigated by means of the fabrication experiment using the low-purity Pb grains. The results are explained in chapter 3.6.

## 2.2 Experimental conditions of TPD-MS analysis

Figure 1 shows the test section connected to the system of TPD-MS [15]. The Pb metal or the Pb alloy of 100 g (or 1 g) was installed in the test cylinder made of stainless steel. The test cylinder was connected with TPD-MS through some stainless tubes, the filter, the cold trap and the valves. One section of the line was immersed into the water tank at a room temperature, and this section works as

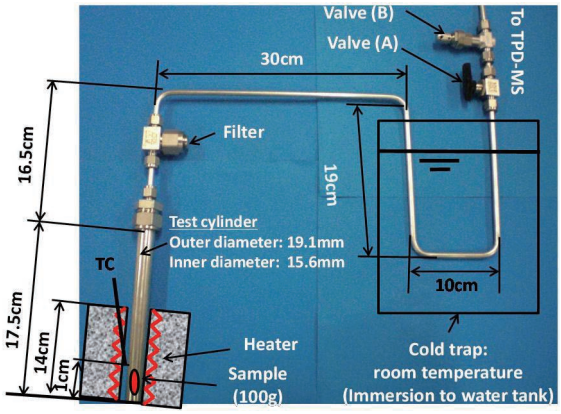


Fig. 1 Test section of TPD-MS.

the cold trap in the test section. The contamination of the system by the evaporated metal from the sample was suppressed by the filter and the cold trap. The test section was the single-use type, and every test was performed using unused test section. The valves (A) and (B) were opened for the evacuation of the TPD-MS system. Then, all the part of the test section was evacuated by a turbo molecular pump at a room temperature, and the pressure reached to $10^{-4}$ Pa. After the evacuation procedure, the temperature of the test cylinder was raised at a rate of 2.5 K/min from a room temperature to 774.5 K. In this procedure, the Pb grains or the ingots of Pb alloys in the cylinder were heated by the heater put on the outside of the cylinder. The surface temperature of the test cylinder was measured by the thermocouple and used for the temperature control.

# 3. Results and Discussion

## 3.1 Chemical behavior of non-metal impurities in Pb metal with purity of 99.9 %

The results of TPD-MS analysis for the low-purity Pb metal and the high-purity one are shown in Figs. 2 (a) and (b), respectively. Figure 2 (c) shows the result of TPD-MS analysis for the Pb-Bi alloy.

$H_2O$ desorption from the low-purity Pb metal is large at the temperature lower than the melting point of Pb (600.7 K) as indicated by the mark of "desorption (I)" in Fig. 2 (a). The $H_2O$ desorption spectrum shows two peaks, which are denoted as Peak-1 (433.3 K) and Peak-2 (524.7 K), respectively. Some small peaks, which are indicated by open diamond (◇) in Fig. 2 (a), appeared at the temperature around the melting point. The previous study

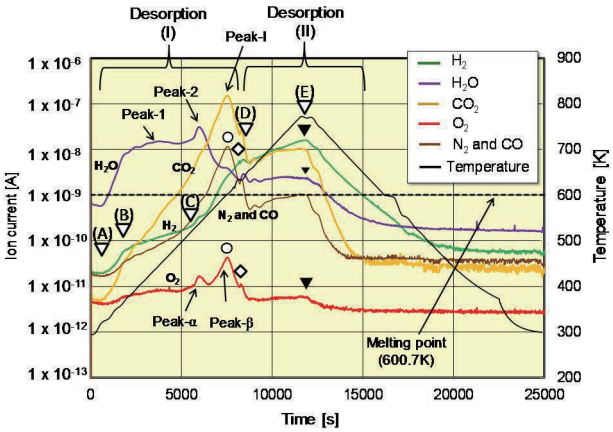


(a) Low-purity Pb metal (quantity: 100 g)

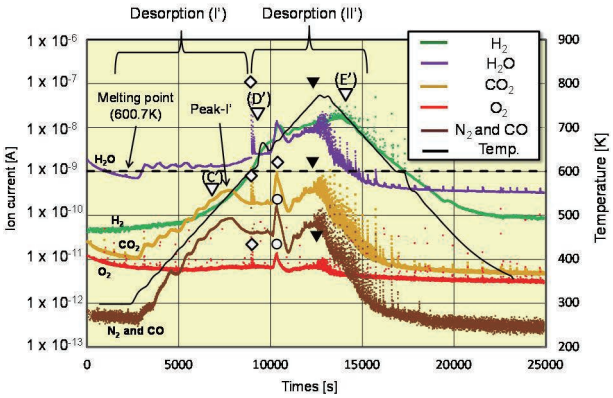


(b) High-purity Pb metal (quantity: 100 g)

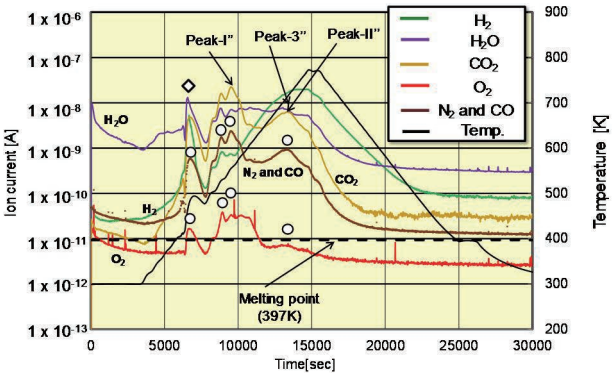


(c) 44.5Pb-55.5Bi alloy (quantity: 100 g)

Fig. 2 Results of TPD-MS experiments (a) metal Pb having purity of 99.9 %, (b) metal Pb having purity of 99.999 %, (c) 45.5Pb-55.5Bi alloy.

[15] indicated that Pb-Li alloy released the non-metal impurities when it transformed from a solid state into a liquid state. Therefore, the peaks marked by the open diamond are due to the release of gas at the phase change of the Pb metal from the solid state to liquid one. The points marked by inverse closed triangle (▼) indicate the slope change according to the temperature curve in Fig. 2 (a). The Peak-1 is likely to be related to desorption of $H_2O$ molecules that are absorbed on the Pb grain surface as Van der Waals adsorption (*i.e.*, physisorbed water) [16]. $H_2O$ desorption is due to the vaporization of the surface water by the heating under the evacuation condition. The Peak-2 is possibly due to desorption of chemisorbed $H_2O$ on the surface of Pb grain or PbO layer formed on the grains. These results indicated that the surface water on the Pb grains can be removed by the baking procedure at the temperature lower than the melting point (600.7 K). As for the low-purity Pb grains, the PbO layer was formed on their surface. $H_2O$ may be absorbed by the PbO layer and transformed to the lead hydroxide ($Pb(OH)_2$) as reported in the previous study [10]. This chemical reaction is expressed as;

$$PbO + H_2O \leftrightarrow Pb(OH)_2. \quad (1)$$

This chemical reaction is reasonable to explain the results in the current work, since the quantity of $H_2O$ stored on the low-purity Pb grains, which have the PbO layer on their surface, was larger than those of the high-purity Pb grains, which does not have the layer (Fig. 2 (b)).

Large desorption of $H_2O$ was detected even at the temperature higher than the melting point. This result indicated that $H_2O$ might be dissolved in the matrix of Pb metal.

$CO_2$ desorption from the solid Pb was also detected, and indicated the presence of $CO_2$ on the grain surface. $CO_2$ desorption at the temperature around 400 K must be due to the release of chemisorbed $CO_2$ on the grain surface. The $CO_2$ desorption spectrum clearly shows the peak, which is denoted as "Peak I" at 588.9 K in Fig. 2 (a). This peak is due to the decomposition of $PbCO_3$, since the decomposing temperature of $PbCO_3$ was 588 K and agreed well with the temperature of the Peak I. The decomposition reaction is expressed in the equation of;

$$PbCO_3 \rightarrow PbO + CO_2. \quad (2)$$

This result indicated that $CO_2$ was mainly contained in the PbO layer on the surface of Pb grains as the chemical form of $PbCO_3$.

Desorption of $H_2O$ and $CO_2$ from the Pb metal was also detected at the temperature higher than the melting point of Pb as indicated by the mark of "desorption (II)" in Fig. 2 (a). The quantity of the desorbed $H_2O$ and $CO_2$ from the liquid Pb was smaller than those from the solid Pb. This result indicated that the quantity of $H_2O$ and $CO_2$ dissolved in the metal matrix is less than that adsorbed on the surface. It is not reasonable to think that $H_2O$ and $CO_2$ molecules moved in the Pb matrix as the chemical form of molecule, and were released from the surface. Their release mechanism might be as they condensed and formed small bubbles in the liquid Pb, and the bubbles transferred and escaped from the melt.

The Gibbs standard free energies for the formation of oxides are summarized in Fig. 3. $H_2O$ and $CO_2$ are chemically stable more than lead oxide (PbO). The oxidation reaction of Pb by these molecules must be negligibly small.

Desorption spectrum of $O_2$ shows two small peaks, which are denoted as "Peak-$\alpha$ (524.2 K)" and "Peak-$\beta$ (590.7 K)". The largest peak in desorption spectrum of CO and $N_2$ were also recognized near the peak-$\beta$. The peaks

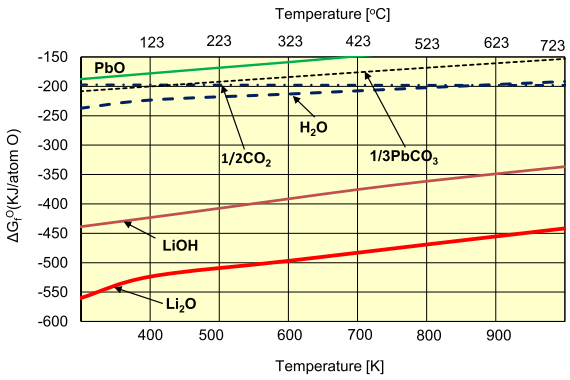


Fig. 3 Gibbs Standard free energy for formation of PbO, $PbCO_3$, $CO_2$ $H_2O$, LiOH and $Li_2O$.

in desorption spectrum of CO and $N_2$ are observed at the same temperatures with those of $CO_2$ and $O_2$. These results indicated that some peaks appeared in these spectrums marked by open circle (○) must be influenced by the detection of the cracking fragment of $CO_2$, which was made by the electron bombardment at the QMS. The PbO lead oxide must not be reduced only by the heating under the evacuation condition. The oxygen trapped as $O_2$ molecule in Pb must be small, since the $O_2$ may react with Pb and form PbO [9]. The locations of the "Peak-α" is close to that of the "Peak-2" of $H_2O$ desorption spectrum. One of the possible reasons for desorption of $O_2$ is due to the dissociation of $H_2O$ molecule, which are contained in the Pb grains. The dissociation reaction might be caused by the capture and the solid solution of hydrogen on the surface of Pb. The chemical reactions are expressed as follows;

$$H_2O(g) \rightarrow 2\,H_{[\text{dissolution in Pb}]} + 1/2O_2(g)\uparrow. \qquad (3)$$

The spectrum of $H_2$ desorption shows a trend to increase with the temperature. The Gibbs standard free energy for formation of PbH is $\Delta G^{O}_{f,PbH} = 209$ kJ/mol at the room temperature. Therefore, the hydride of Pb (*i.e.*, PbH) is chemically unstable. It is unlikely to think $H_2$ desorption is due to the decomposition of PbH (gas) released from the surface of grains. Hydrogen must be trapped in the matrix of metal Pb like a solid solution, and the trapped hydrogen can be released from the surface by increasing the temperature. The slope of the curve in $H_2$ desorption spectrum changed at the five points indicated by open inverse triangles (∇) in Fig. 2 (a). The slope of the curve between the points (A) and (B) is close to that of the $H_2O$ desorption curve. Then, the slope changed as the same as that of $H_2O$ between the points (B) and (C). The slope became larger and close to that of the $CO_2$ desorption spectrum after the point (C). The slope became smaller after the point (D), and this trend is close to that of desorption spectrum of $H_2O$ and $CO_2$, and then became a negative according to the temperature decreasing after the point (E). These trends indicated that the release of $H_2$ is influenced by the release of $H_2O$ and/or $CO_2$ from the surface of Pb grain. One possibility is $H_2$ desorption due to the dissociation of $H_2O$. The dissociation of $H_2O$ might be caused by the dissolution of oxygen in the liquid Pb according to the strong chemical affinity between Pb and oxygen. The reaction is expressed as;

$$H_2O(g) \rightarrow O_{[\text{dissolution in Pb}]} + H_2(g)\uparrow. \qquad (4)$$

Another possibility is $H_2$ desorption according to the formation of $PbCO_3$ from Pb, $CO_2$ and $H_2O$. The chemical reaction is expressed in the equation of;

$$Pb + CO_2(g) + H_2O(g) \rightarrow PbCO_3 + H_2(g)\uparrow. \qquad (5)$$

The change of Gibbs standard free energy for formation in Eq. (5) is estimated as $\Delta G^{O}_{r} = 56.7$ kJ/mol at 600 K, and indicated the possibility of the hydrogen generation. $PbCO_3$ formed in Eq. (5) must be decomposed according to the reaction in Eq. (2).

Almost all the peaks in desorption spectrum of CO and $N_2$ are observed at the same temperature with those in $CO_2$ desorption spectrum. The desorption spectrum of CO and $N_2$ indicates the detection of the cracking fragments of $CO_2$. Therefore, desorption of $N_2$ from the low-purity Pb must be negligibly small.

### 3.2 Chemical behaviors of non-metal impurities in Pb metal with purity of 99.999 and Pb-Bi alloy

Figure 2 (b) shows desorption spectrum for the Pb metal having a purity of 99.999 %. The quantity of $H_2O$ and $CO_2$ desorbed from the high-purity Pb grains was much smaller than that from the low-purity Pb grains. The difference was remarkable especially in the period of "Desorption (I')" in Fig. 2 (b), which corresponds to that of "Desorption (I)" in Fig. 2 (a). The peaks detected in the TPD-MS measurement for the low-purity Pb, which were indicated as "Peak-1" and "Peak-2" in Fig. 2 (a), were not detected for the high-purity Pb. This feature indicates that there was small physisorbed and chemisorbed $H_2O$ on the surface of high-purity Pb grains. The difference was due to the presence of PbO layer on the low-purity Pb grains.

The spectrum for $CO_2$ desorption shows the peak located at the temperature of 553.5 K as indicated by Peak I' in Fig. 2 (b). The peak, which was detected at 588.9 K in the case of low-purity Pb grains, was not detected. The reason is since the PbO layer, which is necessary for the formation of $PbCO_3$, was not formed on the surface of the high-purity Pb grains. However, a certain amount of $CO_2$ was dissolved in the Pb matrix.

The trend of $H_2$ desorption spectrum is similar to that of the low-purity Pb metal, though there are only three points for the slope change in the curve (indicated by the open triangle (∇) as the points C', D' and E' in Fig. 2 (b)). The points corresponding to the points (A) and (B) for the low-purity Pb were not detected. The reason for less points of the slope change is because desorption of $H_2O$ and $CO_2$

from the high-purity Pb in the temperature range of Desorption (I') was much smaller than that from the low-purity Pb.

The desorption spectrums of $H_2O$, $CO_2$ and $O_2$ commonly show the peaks at the temperatures of 603.5 K and 669.5 K as indicated by the mark of open diamond (◇) in Fig. 2 (b). These peaks may be due to the release of the gas by the phase change of the Pb metal. The peaks in the desorption spectrum of $O_2$ and CO marked by (○) must be made by the detection of the cracking fragments of $CO_2$ (i.e. $O_2$ and CO), which were made by the electron bombardment at the QMS.

The results of TPD-MS analysis for the Pb-Bi alloy are shown in Fig. 2 (c). The spectrums for $H_2O$, $CO_2$, $H_2$ and $O_2$ show common peak located at the temperature around the melting point of the Pb-Bi alloy (397 K). The peak was indicated by the mark of open diamond (◇) in Fig. 2 (c). This peak is probably due to the release of the non-metal impurity by the phase change of the Pb-Bi alloy as the same as that for the Pb metal. However, the peak is larger than that detected in Pb. The desorption trend of the non-metal impurities is the similar to that of the Pb metal.

### 3.3 Chemical behavior of non-metal impurities in Pb-Li alloys

The desorption spectrum for the type (A) Pb-17Li alloy is shown in Fig. 4 (a). $H_2O$ and $CO_2$ desorption from Pb-17Li alloy had the spectrum, which was significantly different from that of the pure metal Pb. $H_2O$ and $CO_2$ desorption was much smaller than that from the Pb. The eutectic point of Pb-Li alloy is 508 K, and the liquidus temperature of the Pb-17Li is 511 K [12, 17]. The desorption spectrum of $H_2$, $H_2O$, $CO_2$ and $O_2$ commonly shows two peaks located around the eutectic point and the liquidus temperature, and these peaks are indicated by closed triangle (▼) in Fig. 4 (a). These peaks are due to the release of the gas by the phase change of the Pb-17Li alloy from a solid phase to a liquid one at the liquidus temperature. $H_2$ desorption was much larger than that from the metal Pb. In desorption spectrum of CO and $N_2$, some small peaks were observed around the eutectic point. The peak marked as Peak-$L_{CN}$1 was observed at 702.9 K.

The result of TPD-MS analysis for the Pb-28Li alloy is shown in Fig. 4 (b). The eutectic point of the Pb-28Li alloy is 508 K, and the liquidus temperature of the Pb-28Li alloy is 618 K [12, 17]. Large quantity of hydrogen was released from the alloy. The hydrogen was released from the alloy immediately after the alloy started to melt at the eutectic point. The $H_2$ desorption was large in the temperature range between 325 K and 600 K. The peak was clearly detected around the eutectic point as marked by Peak-L1'. The primary crystals of PbLi precipitated in the matrix were not melted at this instant. Total quantity of $H_2$ desorbed from the Pb-28Li is smaller than that of the type (A) Pb-17Li alloy. In desorption spectrum for CO and $N_2$, some small peaks were observed around the eutectic point.

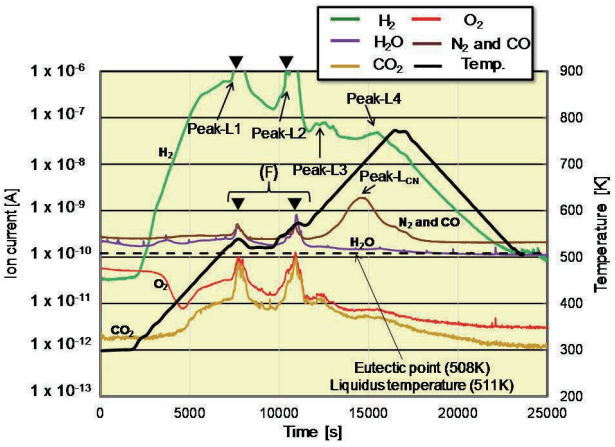


(a) Pb-17Li alloy (Type (A)) (quantity: 100 g)

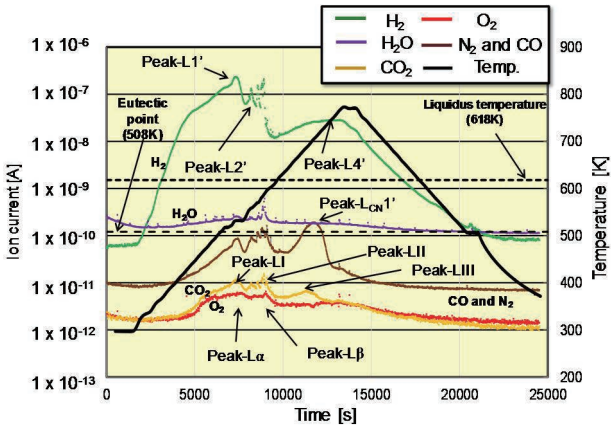


(b) Pb-28Li alloy (Type (A)) (quantity: 100 g)

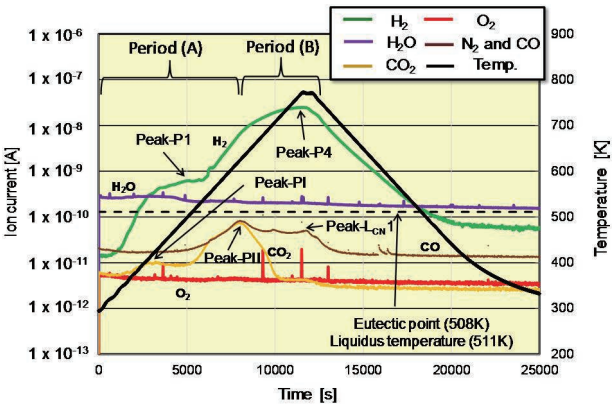


(c) Pb-17Li alloy (Type (B)) (quantity: 1 g)

Fig. 4 Result of TPD-MS analysis for (a) type (A) Pb-17Li, (b) type (A) Pb-28Li and (c) type (B) Pb-17Li fabricated after baking procedure for Pb grains.

The peak marked as Peak-$L_{CN}$1' was observed at 705.9 K. The temperature for this peak was almost the same with that observed in the results obtained from the test with the type (A) Pb-17Li.

The oxygen potential in the Pb-Li alloys is much lower than those of Pb and Pb-Bi because the potential is determined by the chemical activity of Li dessolved as the alloying element in the alloy [13]. The thermodynamic stability of the chemical compounds in the Pb-Li alloy has been discussed in the previous study [18]. The non-metal

impurities such as $O_2$, $N_2$, $H_2O$, CO and $CO_2$ react with the Pb-Li alloy. The possible chemical reactions are listed as follows;

$$1/2\,H_2O(g) + Li_{[alloy]} \rightarrow LiH + 1/2O_2(g)\uparrow, \quad (6)$$

$$H_2O(g) + Li_{[alloy]} \rightarrow LiOH + 1/2\,H_2(g)\uparrow, \quad (7)$$

$$H_2O(g) + 2Li_{[alloy]} \rightarrow LiOH + LiH, \quad (8)$$

$$LiH \rightarrow Li_{[alloy]} + 1/2\,H_2(g), \quad (9)$$

$$CO_2(g) + 2Li_{[alloy]} + 1/2O_2 \rightarrow Li_2CO_3, \quad (10)$$

$$CO_2(g) + 2Li_{[alloy]} \rightarrow Li_2O + CO(g)\uparrow, \quad (11)$$

$$CO(g) + 2Li_{[alloy]} \rightarrow Li_2O + C, \quad (12)$$

$$O_2(g) + Li_{[alloy]} \rightarrow Li_2O, \quad (13)$$

$$1/2O_2(g) + Pb_{[alloy]} \rightarrow PbO, \quad (14)$$

$$1/2N_2(g) + 3Li_{[alloy]} \rightarrow Li_3N, \quad (15)$$

$$Li_3N + 3\,H_2O(g) \rightarrow 3LiOH + NH_3(g)\uparrow, \quad (16)$$

$$NH_3(g) \rightarrow 1/2N_2 + 3/2\,H_2(g)\uparrow. \quad (17)$$

The change of the Gibbs standard free energy (*i.e.*, $\Delta G_r^o$) considering the activity of Li in the Pb-Li alloy is expressed as

$$\begin{aligned}\Delta G_r &= \Delta G_{f,(products)} - \Delta G_{f,(reactants)} \\ &= \Delta G_{f,(products)} - \Delta G_{f,(H2OorCO2)} - RT\ln(a_{Li}).\end{aligned} \quad (18)$$

The chemical activity of Li and Pb (i.e., $\alpha_{Li}$ and $\alpha_{Pb}$) in the alloy is summarized in ref. [13], and the equations are expressed as follows;

$$\begin{aligned}\ln(\alpha_{Li}) = &-19.48x_{Li}^3 + 21.42x_{Li}^2 - 1.366x_{Li} - 0.5794 \\ &+ \frac{20350x_{Li}^3 - 22220x_{Li}^2 + 9711x_{Li} - 7840}{T},\end{aligned} \quad (19)$$

$$\begin{aligned}\ln(\alpha_{Pb}) = &-3.291x_{Li}^3 + 2.044x_{Li}^2 - 1.755x_{Li} + 0.04122 \\ &+ \frac{652.7x_{Li}^3 - 1270x_{Li}^2 + 281.6x_{Li} - 15.02}{T}.\end{aligned} \quad (20)$$

$\Delta G_r$ for the reactions of eqs. (6 - 12) for the case of Pb-17Li are evaluated according to the equation (18) with the thermodynamic database MALT 2 code. The chemical activity of Li in the Pb-17Li alloy at 500 K is $1 \times 10^{-6}$ by the equation (19). $\Delta G_r$ are summarized in Fig. 5. The change of the Gibbs free energy for the chemical reaction of eq. (6) is small, though the value is positive. Therefore, it is reasonable not to exclude the reaction of eq. (6). The other chemical reactions of eqs. (7 - 12) are caused even at the low temperature. Therefore, the molecules of $O_2$, $H_2O$ and $CO_2$ must react with Li in the alloy, and then oxygen must dissolve in the alloy as the chemical forms of $Li_2O$, LiOH and $Li_2CO_3$. In the same time, hydrogen dissolves as the

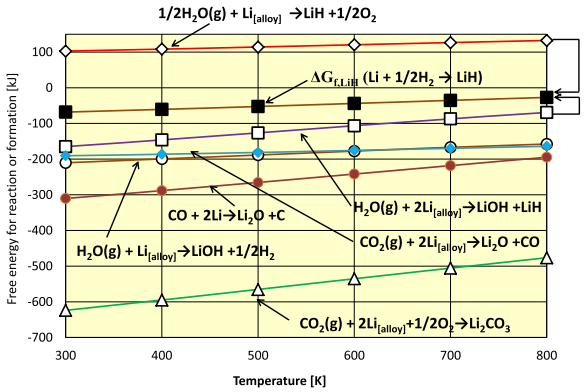


Fig. 5 Free energy for reaction and formation of non-metal impurity in Pb-17Li alloy.

form of atom, molecule and chemical compounds such as LiH and LiOH into the alloy.

Desorption spectrum of CO and $N_2$ in the test with type (A) Pb-17 Li and Pb-28Li indicated the release of CO and/or $N_2$ was large around the temperature of 508 K and 700 K. CO could generate according to the equation (11). Then, CO may not react with Li according to the equation (12), if neighboring Li atoms already reacted and formed $Li_2O$. Then, CO must be dissolved in the alloy. CO might be released from the alloy, when the alloy was melted at the eutectic point. Nitrogen must be dissolved in Li according to the equation (15). $Li_3N$ is not chemically stable at the temperature around 700 K. Then, $Li_3N$ may be decomposed and nitrogen must be released from the alloy. Ammonia ($NH_3$) might be formed by the reaction between $Li_3N$ and $H_2O$ during the fabrication procedure according to the reaction of equation (16). $NH_3$ can be decomposed at the high temperature around 700 K in the reaction of equation (17). Desorption spectrum of $H_2$ in the test with Pb-17Li (type (A)) and Pb-28Li (type (A)) indicate the increase of hydrogen desorption around the temperature of 700 K. This desorption might be based on the chemical reaction expressed in equation (17).

## 3.4 Hydrogen desorption from Pb-Li alloys

The Pb grains, which contained $H_2O$ as explained in chapters 3.1 and 3.2, were used for the fabrication of Pb-Li alloys [3]. Then, the large quantity of $H_2$ and LiH molecules must be generated according to the chemical reactions between Li and $H_2O$. The possible chemical reactions were already expressed in the equations (6 - 8). The Gibbs standard free energy for formation of LiH is shown as closed square (■) in Fig. 5. LiH is not chemically stable and must be decomposed at high temperature according to the reaction of eq. (9). Then, hydrogen atom might be recombined on the surface of the Pb-Li alloys, and hydrogen molecules were released from the surface.

$H_2$ desorption from the solid Pb-17Li alloy was detected shortly after the start of the heating up of the sample. This behavior was not observed for the tests with the Pb metal and the Pb-Bi alloy. The temperature of the type (A)

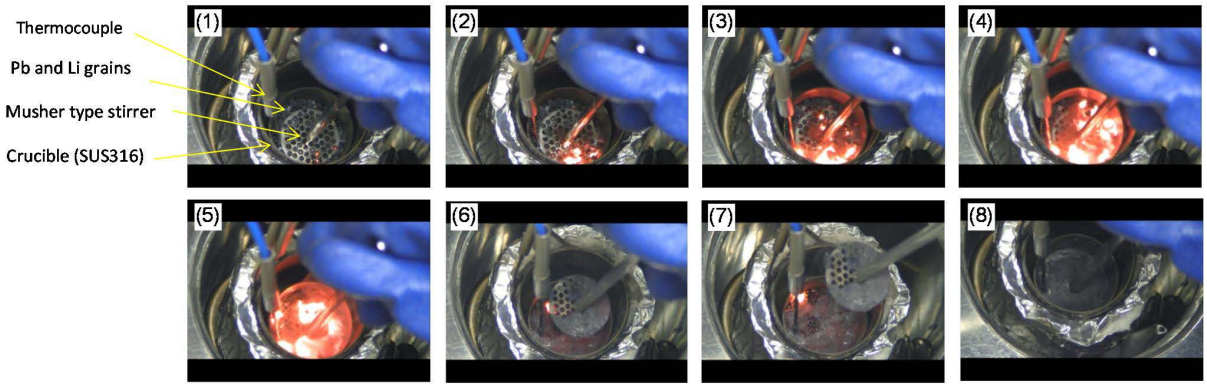


Fig. 6 Explosive flame generation during fabrication procedure of Pb-17Li alloy using low-purity Pb grains [12].

Pb-17Li alloy was constant as indicated by "region (F)" in Fig. 4 (a), when the large amount of hydrogen was released from the alloy. These features indicated that $H_2$ desorption from the solid Pb-Li alloy could be based on endothermic reaction. The possible reaction is expressed as follows;

$$\text{Pb-Li} - \text{H} \rightarrow \text{Pb-Li} + 1/2\,\text{H}_2 \uparrow . \qquad (21)$$

The enthalpy change for the decomposition of Pb-Li-H is not made clear. However, that for the decomposition of LiH is $\Delta H = 95.1$ kJ/mol. Therefore, it is possible to think the standard enthalpy for the decomposition of Pb-Li-H is positive and the chemical reaction of eq. (21) is endothermic reaction.

## 3.5 Effect of baking procedure for Pb grains on purity control of Pb-Li alloy in fabrication procedure

Figure 4 (c) shows the TPD spectrum for the type (B) Pb-17Li, which was fabricated after the baking procedure for the low-purity Pb grains. The trend of $H_2$ desorption from the alloy in the period (A) was significantly different from that of the type (A) alloy fabricated without the baking procedure. The spectrum of $H_2$ desorption does not have the peaks corresponding to the peak-L1 and the peak-L2 for type (A) Pb-17Li and the peak-L1' and the peal-L2' for type (A) Pb-28Li. However, the quantity of $H_2$ desorbed from the type (B) alloy in the period (B) was almost the same with that from the type (A) Pb-28Li alloys, though the sample quantity used was one hundredth of that used for the test of the type (A) alloy. $H_2$ desorption from the type (B) alloy indicated that a certain quantity of $H_2$ was dissolved in the matrix of the alloy. The dissolution was possibly due to the formation of LiH by the chemical reaction between the Li and $H_2O$, which were contained in the matrix of the low-purity Pb. The result indicated that the removal of $H_2O$ from the surface of the Pb grains by the baking procedure contributed to suppress the supply of $H_2O$ to the unintended chemical reaction in the fabrication procedure. It was indicated that $H_2O$ absorbed on the surface of Pb grains contributed the formation of LiH on the surface of Pb-Li alloy.

## 3.6 Discussions on chemical behaviors of non-metal impurities in the fabrication procedure of Pb-Li alloys

Figure 6 shows that the flame having a red color was generated during the fabrication experiment, in which the Pb-17Li alloy was fabricated from the Pb grains having a purity of 99.9 %. The baking procedure for the low-purity Pb grains was not performed. This experiment was performed inside the glove box filled with high-purity Ar (99.999 %). The result provides the evidence for the hydrogen formation and dissolution to the alloy by the chemical reactions according to the equations (6 - 8, 15 - 17). The flame was generated at the instant when the melting Li grains were pressed to the surface of the melting Pb grains by the musher type stirrer [12] at 623 K (Fig. 6 (2)). In this instant, the molten Li might react with $H_2O$ and PbO (or $PbO_2$), which were contained on the surface of the Pb grains. The chemical reactions between PbO (or $PbO_2$) and the heat for the oxidation of Li at 700 K [19] are expressed as follows;

$$2\text{Li} + \text{PbO} \rightarrow \text{Li}_2\text{O} + \text{Pb} + 386.139\,\text{kJ}, \qquad (22)$$

$$4\text{Li} + \text{PbO}_2 \rightarrow 2\text{Li}_2\text{O} + \text{Pb} + 933.65\,\text{kJ}. \qquad (23)$$

The heat generation by the chemical reaction between Li and $H_2O$, which is expressed by eq. (7), is given as 240.7 kJ at 700 K. The heat must be generated by the chemical reaction locally at the interface between the Li grain and the low-purity Pb grain. The heat by the chemical reactions is larger than that for the formation of Pb-Li alloy. Therefore, the ignition of Li was not observed when the high-purity Pb grains were used for the fabrication of Pb-Li alloys [12]. The heat was used for the temperature increasing of Li and its ignition. The ignition area expanded according to the increase of the contact area of the grains by being pushed with the musher type stirrer (Figs. 6 (3 - 5)). The small explosive flame was continuously created as shown in Figs. 6 ((6) and (7)). After the mixing of the grains (Fig. 6 (8)), the flame generation was not observed.

It was reported in the previous article [20] that the flame having a red color was generated by the chemical reaction between Li and $H_2O$. In the current work, it was

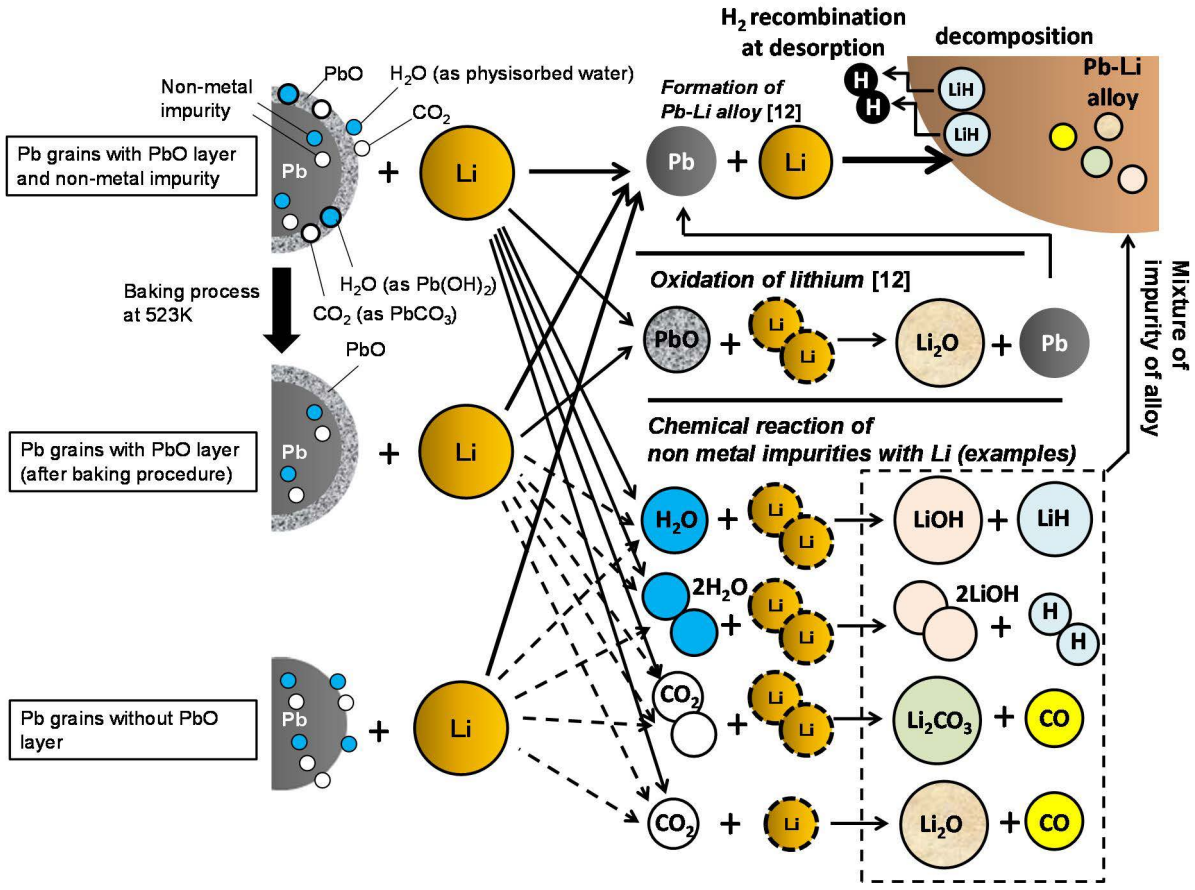


Fig. 7 Mechanism of non-metal impurity mixture into Pb-Li alloy in fabrication procedure of alloy.

clearly shown in Fig. 2 (a) that the large quantity of $H_2O$ was contained on the surface of the low-purity Pb grains. These facts indicated that the flame having a red color was generated by the chemical reaction between Li and $H_2O$ during the mixing procedure of Li and Pb grains.

From these discussions, $H_2$ and/or LiH could be generated by the chemical reaction between the molten Li and $H_2O$ according to eqs. (6 - 8). However, the solubility of hydrogen in Pb-Li alloys is quite small, though that in Li is large [21]. If the quantity of hydrogen generated by the chemical reactions in the fabrication procedure was larger than the solubility in the alloys, the excess hydrogen might be precipitated as $H_2$ molecules, and released to the outside of the alloy. Then, a portion of hydrogen, which was generated by the chemical reaction, was dissolved in the Pb-Li alloy. In this procedure, LiH and/or Pb-Li-H can be formed on the surface of the Pb-Li alloy and in the matrix of the alloy.

Figure 7 shows the chemical behaviors of non-metal impurities in the fabrication procedure of the Pb-Li alloys. $H_2O$ and $CO_2$ react with Li, and then oxygen and hydrogen must be dissolved as the chemical compounds of LiH, LiOH, $Li_2O$ and $LiCO_3$ in the alloy. The quantity of Pb used for the fabrication of type (A) Pb-28Li alloy was smaller than that of type (A) Pb-17Li alloy. In this case, the total quantity of $H_2O$ reacted with Li was also smaller than that in the fabrication of type (A) Pb-17Li alloy. Then, the quantity of hydrogen dissolved in the alloy via the chemical reactions must be smaller. In the current work, $H_2$ desorption from the Pb-28Li alloy is smaller than that from the Pb-17Li alloy. Therefore, the results agreed well with the mechanism for the dissolution of hydrogen. The quantity of $H_2O$ and $CO_2$ dissolved in the Pb-Li alloy is small according to the chemical reactions between the molten Li and the non-metal impurities in the fabrication procedure. This reaction resulted to the small desorption of $H_2O$ and $CO_2$ from the alloy in the TPD-MS measurement.

The baking procedure for the low-purity Pb grains removed the non-metal impurities from the surface of the grains. Then, the baking procedure resulted to suppress the chemical reactions between the molten Li and the non-metal impurities in the fabrication procedure of the alloy as shown in Fig. 7. The suppression of the chemical reactions in the fabrication procedure can result to the fabrication of high-purity Pb-Li alloy.

## 4. Conclusions

The chemical behaviors of the non-metal impurities in the Pb metal and the Pb alloys were experimentally investigated by means of temperature programmed desorption mass spectrometer (TPD-MS) analysis. The TPD-MS analysis was performed in the temperature range between

room temperature and 773 K. Major conclusions are follows;

1. The results of TPD-MS analysis for the Pb metal showed the desorption of $H_2O$ and $CO_2$ from the surface and the matrix. This chemical behavior indicated that these molcules were originally presented on the surface and/or in the matrix of the Pb metal, since these molcules are thermodynamically stable in comparison with the oxygen potential for the formation of lead oxide.
2. The total quantity of $H_2O$ desorbed from the low-purity Pb metal in the TPD-MS analysis was larger than the high-purity metal. The low-purity Pb metal had the layer of PbO on the surface, though the higy purity one did not have the layer. These results indicated that the physical and chemical absorption of $H_2O$ on the surface of Pb metal was promoted by the presence of the PbO layer.
3. The spectrum of $CO_2$ desorption obtained in the TPD-MS analysis for the low-purity Pb metal had a clear peak at the temperature of 588.9 K. This chemical behavior indicated that $CO_2$ was released from the surface of the metal according to the decomposition of $PbCO_3$, which was formed on the surface.
4. Desorption of $H_2O$, $CO_2$, $H_2$ and $O_2$ from 44.5Pb-55.5Bi alloy was detected, and the trend of desorption spectrum was similar to that from pure Pb metal.
5. Desorption of $H_2$ from the Pb metal and the Pb-Bi alloy might be caused by the release of the $H_2$ dissolved in the Pb matrix like a solid solution. The other possible mechanism of $H_2$ desorption is due to the chemical decomposition of $H_2O$, which was released from the metal during the TPD-MS analysis. It is also discussed that $H_2$ generation due to the formation of $PbCO_3$ by the chemical reaction between Pb, $H_2O$ and $CO_2$ on the surface of Pb grains.
6. The quantity of $H_2O$ and $CO_2$ desorbed from the Pb-Li alloys was much smaller than that from pure Pb metal. These molecules are chemically unstable in the Pb-Li alloy. $H_2O$ and $CO_2$ must react with Li in the alloys, and form the chemical compounds such as $Li_2O$ LiOH and LiH. These chemical compounds are stable in the alloy.
7. The total quantity of $H_2$ desorbed from the Pb-17Li and the Pb-28Li alloys was much larger than that from Pb and Pb-Bi alloy. Lithium hydride (LiH) must be formed by the chemical reaction between Li and $H_2O$ in the fabrication procedure of the alloys. LiH might be decomposed by the heating of the alloys in the TPD-MS analysis, and hydrogen was released from the alloy.
8. Baking procedure for the Pb grains was effective to remove $H_2O$ and $CO_2$ from thier surface. The Pb-17Li alloy was fabricated with the low-purity Pb grains after the baking procesure. The quantity of $H_2$ desorbed from the surface of this alloy in the solid state was much smaller than that from the alloy fabricated without the baking procedure.

## Acknowledgement

This work was carried out based on JSPS KAKENHI Grant-in-Aid for Young Scientists (B) 25820437 and National Institute for Fusion Science budget code NIFS14KOBF028. The study on the fabrication of the Pb-Li alloys was partially supported by the Japan Atomic Energy Agency under the Joint Work contract 27K395, as a part of Broader Approach activities.

[1] M. Kondo, M. Takahashi, T. Teruya, V. Tsisar and T. Muroga, Fusion Eng. Des. **87**, 1777 (2012).
[2] M. Kondo and T. Muroga, Plasma Fusion Res. **8**, 3405053 (2013).
[3] M. Kondo, T. Oshima, M. Tanaka, T. Muroga and A. Sagara, Fusion Eng. Des. **87**, 1788 (2012).
[4] S. Fukada, T. Muneoka, M. Kinjyo, R. Yoshimura and K. Katayama, Fusion Eng. Des. **96-97**, 95 (2015).
[5] Q. Xu, M. Kondo, T. Nagasaka, T. Muroga and O. Yeliseyeva, J. Nucl. Mater. **394**, 20 (2009).
[6] V. Tsisar, M. Kondo, Q. Xu, T. Muroga, T. Nagasaka and O. Yeliseyeva, J. Nucl. Mater. **417**, 1205 (2011).
[7] M. Kondo, M. Takahashi, T. Suzuki, K. Ishikawa, K. Hata, S. Qiu and H. Sekimoto, J. Nucl. Mater. **343**, 349 (2005).
[8] M. Kondo, M. Takahashi, N. Sawada and K. Hata, J. Nucl. Sci. Technol. **43**, 107 (2005).
[9] M. Kondo, M. Takahashi, K. Miura and T. Onizawa, J. Nucl. Mater. **357**, 97 (2006).
[10] Handbook on Lead-bismuth Eutectic Alloy and Lead Properties, Materials Compatibility, Thermal-hydraulics and Technologies (2007 edition), OECD-NEA, (https://www.oecd-nea.org/science/reports/2007/nea6195-handbook.html)
[11] G. Alberro, I. Penalva, A. Sarrionandia-Ibarra, F. Legarda and G.A. Esteban, Fusion Eng. Des. **98-99**, 1919 (2015).
[12] Y. Nakajima, M. Kondo and T. Nozawa, Fusion Eng. Des. **98-99**, 2009 (2015).
[13] M. Kondo, Y. Nakajima, M. Tsuji and T. Nozawa, Fusion Eng. Des., inpress (2016). doi:10.1016/j.fusengdes.2015.12.029
[14] M. Kondo and Y. Nakajima, Fusion Eng. Des. **88**, 2556 (2013).
[15] T. Sakabe, T. Yokomine, T. Kunugi, Z. Kawara, Y. Ueki and T. Tanaka, Fusion Eng. Des. **89**, 1417 (2014).
[16] G. Ran, C. Xiao, X. Chen, Y. Gong, C. Kang and X. Wang, J. Nucl. Mater. **466**, 316 (2015).
[17] P. Hubberstey and T. Sample, J. Nucl. Mater. **191-194**, 283 (1992).
[18] P. Hubberstey and T. Sample, J. Nucl. Mater. **199**, 149 (1993).
[19] Thermodynamic database MALT group. Thermodynamic database MALT for Windows. Kagaku Gijutsu-Sha. 2005. (CD-ROM), available from http://www.kagaku.com/malt/index.html (accessed 2016-03-29).
[20] T. Asada, S. Kano, Y. Tachi and M. Kawai, "Properties of Lithium and its handling", JNC TN9410, 2000-013 (2000) (in Japanese).
[21] M. Kondo, T. Oshima, M. Tanaka, T. Muroga and A. Sagara, Fusion Eng. Des. **87**, 1788 (2012).